

Supporting information

Evaluate the Effect of nitrate and chloride on Cd(II)-Induced Cell Oxidative Stress by Scanning Electrochemical Microscopy

Na Pan¹, Liping Lu^{1,2*}, Dongtang Zhang^{2*}, Xiayan Wang²

¹Key Laboratory of Beijing on Regional Air Pollution Control, Department of Environmental Science,
Beijing University of Technology, Beijing 100124, P.R. China;

²Center of Excellence for Environmental Safety and Biological Effects, Department of Chemistry and
Biology, Beijing University of Technology, Beijing 100124, P.R. China

E-mail: lipinglu@bjut.edu.cn; zhangdongtang@bjut.edu.cn

Content

SI-1 Detection diagram	S3
SI-2 Simulation fitting of theoretical approach curve.....	S4
SI-3 Cd(II)-induced changes in cell morphology	S6
SI-4 SECM 2D image of MCF-7 cells.....	S7
SI-5 Quantitative determination of H ₂ O ₂	S8
SI-6 Detection of antioxidant activity and content	S9
SI-7 Detection of intracellular pH.....	S10
SI-8 Detection of intracellular ATP content	S11
SI-9 Detection of intracellular nitrite content	S12
References	S13

SI-1 Detection diagram

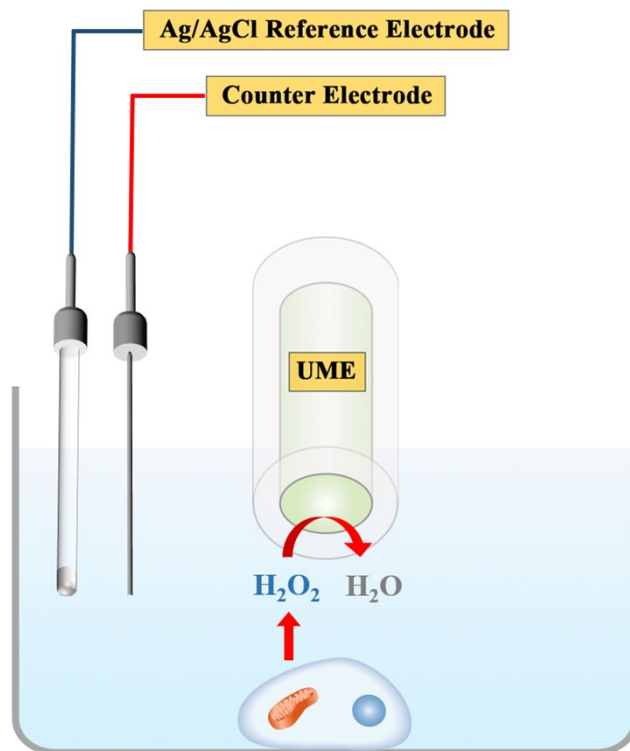


Fig. S1 Diagram of the SECM setup along with a schematic of ROS detection.

SI-2 Simulation fitting of theoretical approach curve

According to the following formulas and the parameters in Table 1, the theoretical approach curve was calculated and plotted. RG of experimental probe is 3. (The approach curves for an insulator actually depend upon r_g , since the sheath around the conducting portion of the electrode blocks diffusion. r_g often expressed in the SECM literature as $RG=r_g/a$, where r_g is the radius of the insulating sheath, a is the radius of Pt probe.) The experimental approach curves were obtained at the blank of petri dishes (no cells) in $1 \times$ PBS containing 1 mM $\text{Ru}(\text{NH}_4)_6\text{Cl}_3$ at -0.35 V. The experimental approach curve was normalized and fitted with the theoretical approach curve. The approach curve showed a negative feedback current because of the insulating substrate, the current decreased with the decreased tip-substrate distance. The actual distance at the intersection of the two curves is the distance between the probe tip and the substrate.

$$I_T \rightarrow I = I_T / I_{T,\infty} \quad (1)$$

$$d_{exp} \rightarrow L = d/a = (d_0 - d_{exp})/a \quad (2)$$

$$I = 1/[A + B/L + C \exp(D/L)] \quad (3)$$

Where, I_T represents the probe tip current. $I_{T,\infty}$ is the tip current at an infinite distance from the substrate. a is the radius of the UME probe, $a = 5 \mu\text{m}$ in the experiment. d is the distance between the tip and substrate distance. d_0 is the distance between the initial scanning position the first and substrate. d_{exp} is the distance the probe scans downward.

Table S1 Parameter Values for formula (3) (Negative Feedback) at different RG Values¹

RG	A	B	C	D
10.2	0.40472	1.60185	0.58819	-2.37294
8.13	0.42676	1.46081	0.56874	-2.28548
5.09	0.48678	1.17706	0.51241	-2.07873
3.04	0.60478	0.86083	0.39569	-1.89455
2.03	0.76179	0.60983	0.23866	-2.03267

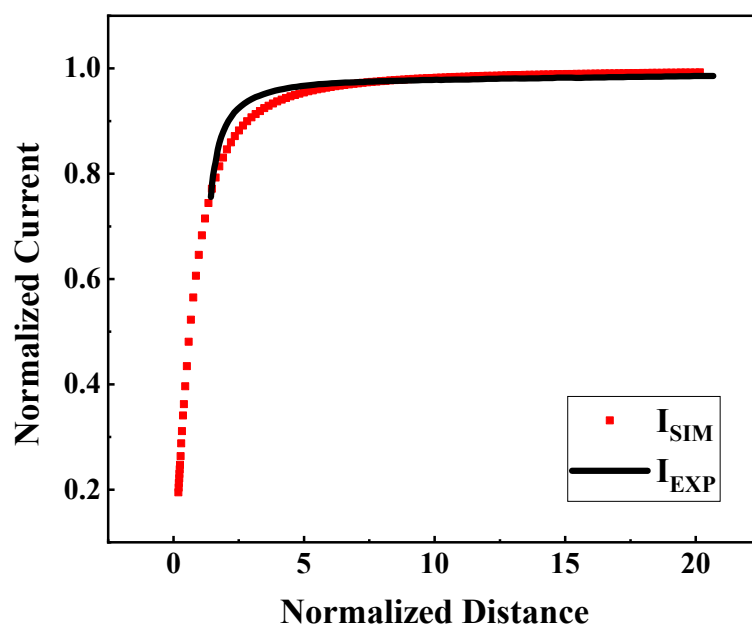


Fig. S2 The approach curves of 10 μM Pt electrodes at -0.35 V in $1\times\text{PBS}$ solution containing $1\text{mM Ru}(\text{NH}_3)_6\text{Cl}_3$ over petri dish.

After the specific location of MCF-7 cells was determined according to 2D image, the probe was lifted $200\ \mu\text{m}$ at the blank of petri dish and was moved to the center of MCF-7 cells. Then, the approach curve above the center of MCF-7 cell was obtained. Because of the impermeability of $\text{Ru}(\text{NH}_4)_6\text{Cl}_3$, the distance between the terminal point of approach curve and cell was equal to the distance of tip-to-substrate. Therefore, the difference between the lifted height ($200\ \mu\text{m}$) and the descent height is the height of MCF-7 cell.

SI-3 Cd(II)-induced changes in cell morphology

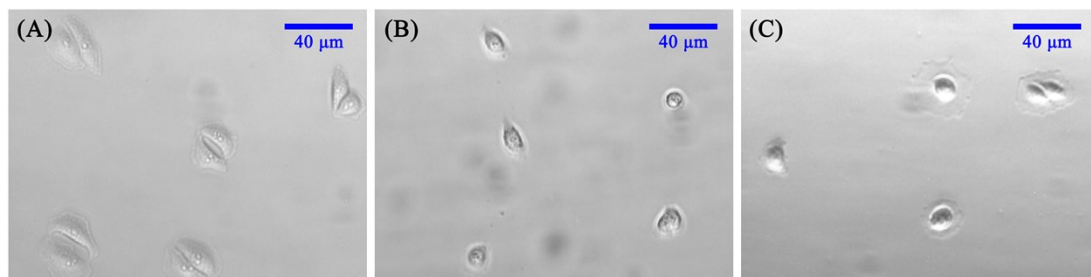


Fig. S3 Optical microscopic pictures of MCF-7 cells incubated with (A) 0, (B) 50, (C) 80μM CdCl₂ for 2 h

As shown in Fig. S3A, under normal physiological conditions, the morphology of MCF-7 cells were fusiform and clearly delineated. With the increasing of incubated concentration, the cells morphology became round gradually.

SI-4 SECM 2D image of MCF-7 cells

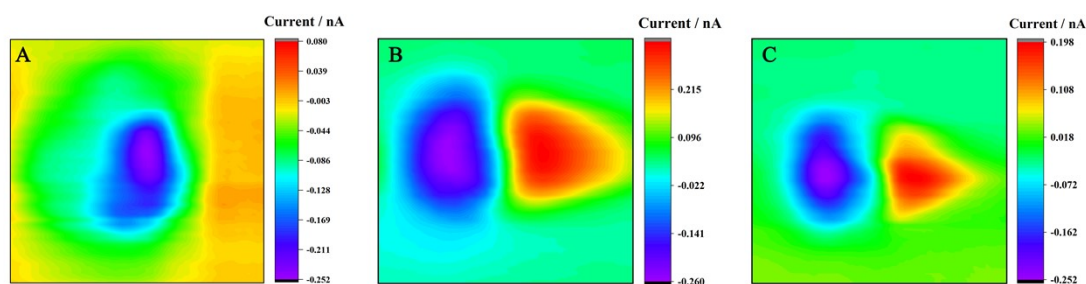


Fig. S4 SECM 2D image of MCF-7 cells incubated with (A) 20, (B) 60, (C) 80 μM CdCl₂ for 2 h. The scanning rate was 10 μm/s, tip-substrate distance is 12 μm approximately, number of samples is 5/μm.

When the probe passed over the cells, the distance between tip and substrate decreased, leading to a reduction of the diffusion current. Under the stimulation of Cd²⁺, H₂O₂ released from MCF-7 cells and was reduced at tip, leading to an increasing current. In Fig. S4, the blue part represented a drop in current and the red part represented an increasing current. There was almost no current increased when the cell incubated with 20 μM CdCl₂. As shown in Fig. S4B, the current increased significantly which indicated that a large amount of ROS released. When incubated with 80 μM CdCl₂, the generation of ROS reduced.

SI-5 Quantitative determination of H₂O₂

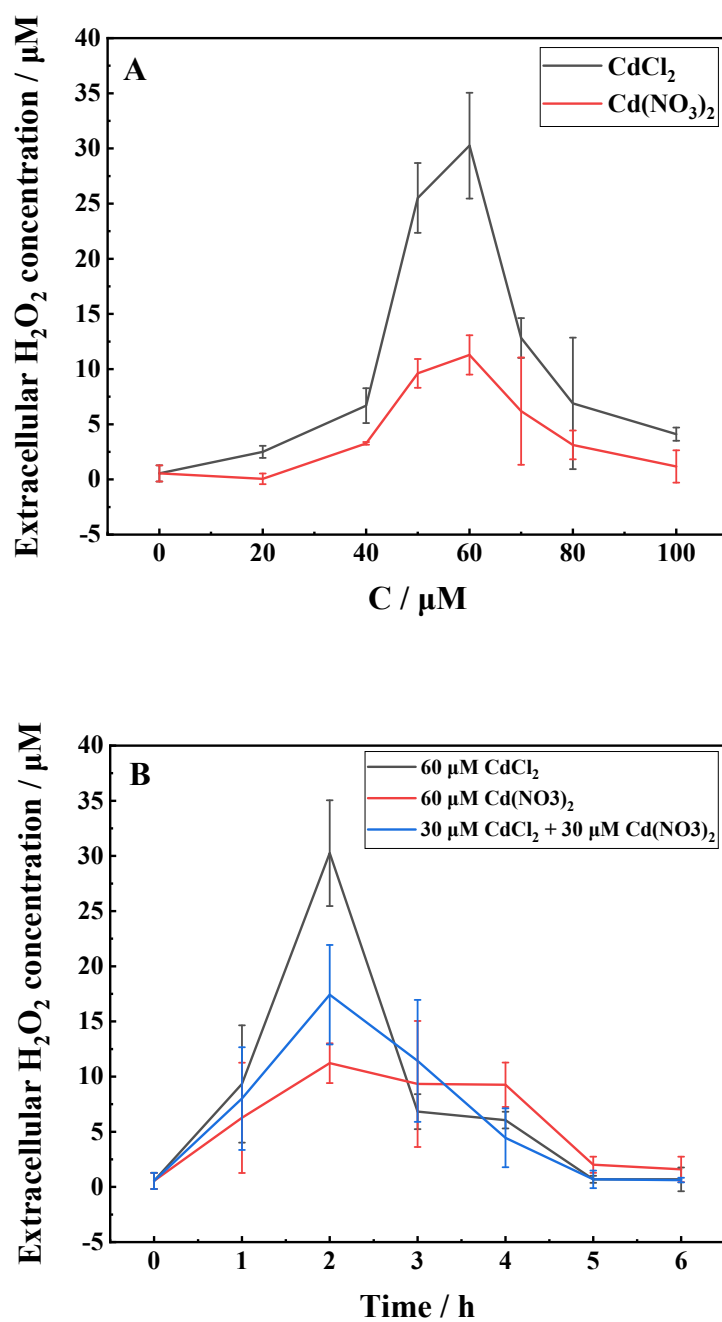


Fig. S5 Extracellular H₂O₂ concentration after incubation (A) in different concentration of Cd²⁺ for 2 h. (B) in 60 μM Cd²⁺ for different time.

SI-6 Detection of antioxidant activity and content

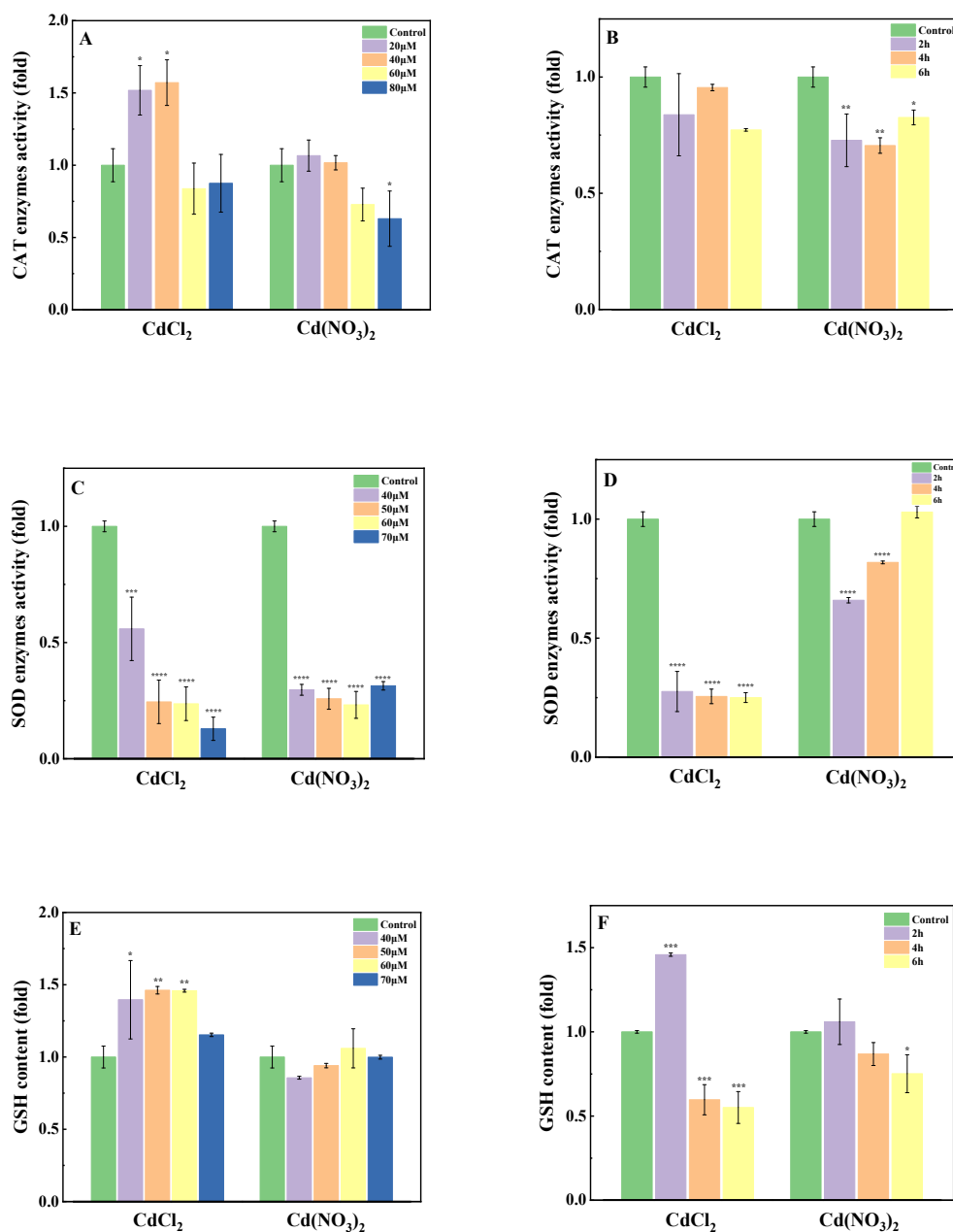


Fig. S6 The activity of (A) CAT, (C) SOD and (E) GSH content of MCF-7 cells after incubation in different concentrations of CdCl₂ or Cd(NO₃)₂ for 2h. The activity of (B) CAT, (D) SOD and (F) GSH content after incubation in 60 µM CdCl₂ or Cd(NO₃)₂ for different time. *P < 0.05, **P < 0.005, ***P < 0.001, ****P < 0.0001; Significant differences compared with control and tested by repeated measured ANOVA with Tukey's multiple comparison; Data are mean ± S.D. (n = 3).

SI-7 Detection of intracellular pH

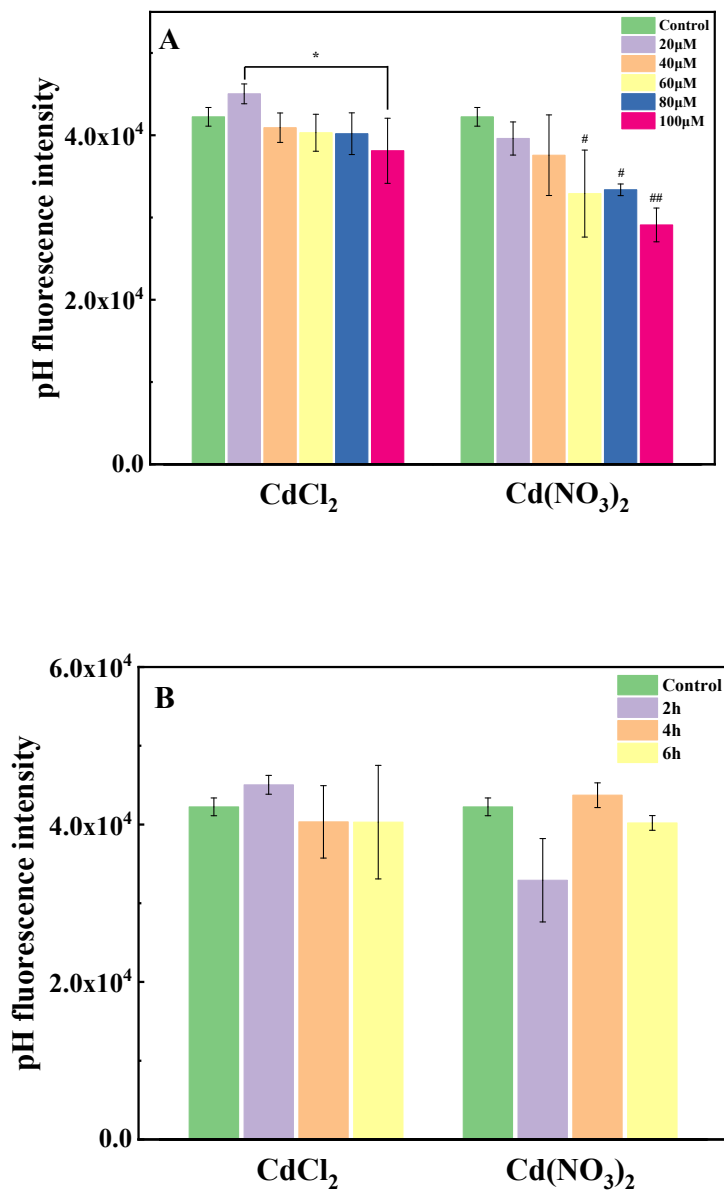


Fig. S7 pH fluorescence intensity of MCF-7 cells after (A) incubation in different concentrations of CdCl₂ or Cd(NO₃)₂ for 2h and (B) incubation in 60 μM CdCl₂ or Cd(NO₃)₂ for different time.

*P < 0.05; #P < 0.05 and ##P < 0.005 compared with control and tested by repeated measured

ANOVA with Tukey's multiple comparison; Data are mean ± S.D. (n = 3).

SI-8 Detection of intracellular ATP content

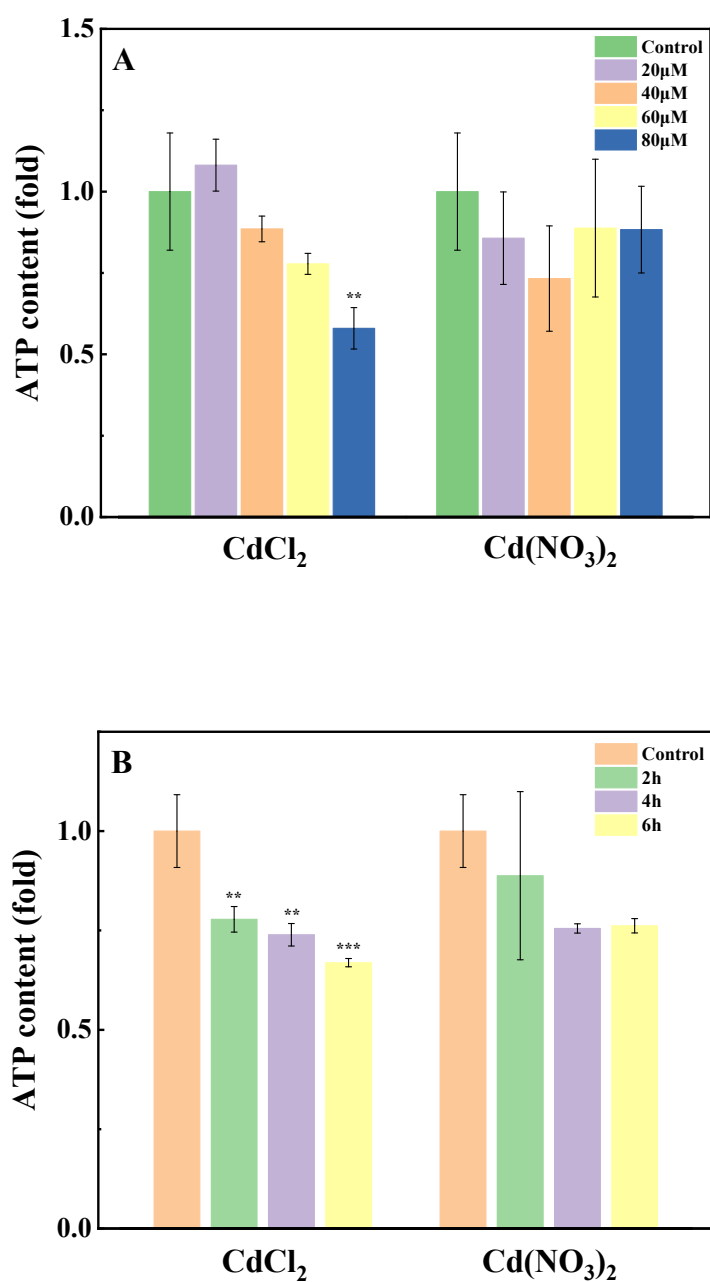


Fig. S8 ATP production of MCF-7 cells after (A) incubation in different concentrations of CdCl₂ or Cd(NO₃)₂ for 2h and (B) incubation in 60 μ M CdCl₂ or Cd(NO₃)₂ for different time. **P < 0.005 and ***P < 0.001 compared with control and tested by repeated measured ANOVA with Tukey's multiple comparison; Data are mean \pm S.D. (n = 3).

SI-9 Detection of intracellular nitrite content

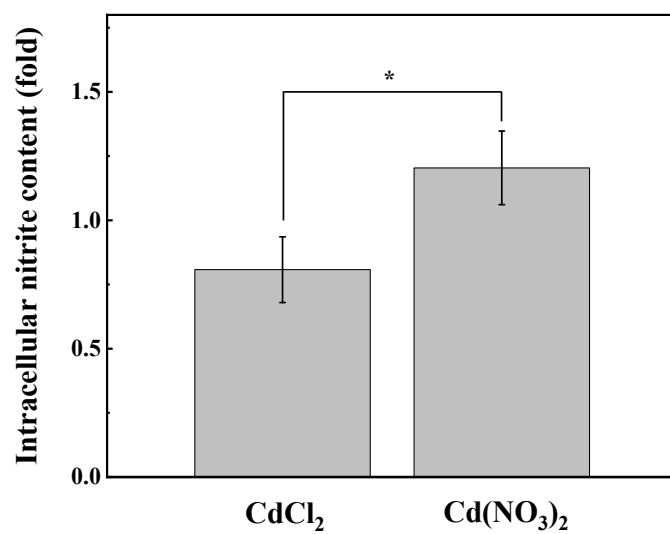


Fig. S9 Intracellular nitrite content of MCF-7 cells incubated with 60 μM CdCl₂ or Cd(NO₃)₂ for 2 h. *P < 0.05; Data are mean ± S.D. (n = 3).

References

- 1 J. Bard and M. V. Mirkin, *Scanning electrochemical microscopy, second edition*, CRC press, Boca Raton, 2012.
- 2 J. Bard, X. Li, W. Zhan, Chemically imaging living cells by scanning electrochemical microscopy. *Biosensors and Bioelectronics*, 2006, 22, 461-472.
- 3 Fan, X., Lu, L., Kang, T. Investigation on Real-time Release of Reactive Oxygen Species from Cells Based on Scanning Electrochemical Microscopy. *Journal of Instrumental Analysis*, 2019, 38(04), 379-384. (in Chinese)
- 4 Zhang, B., Pan, N., Fan, X., Lu, L., Wang, X. Real-time effects of Cd(II) on the cellular membrane permeability. *Analyst*, 2021, 146, 5973-5979.